Journal of Modern Optics

ISSN: 0950-0340 (Print) 1362-3044 (Online) Journal homepage: http://www.tandfonline.com/loi/tmop20

Correction of amplitude distortions for truncated Bessel beam and SER estimation for 4ASK

Halil T. Eyyuboğlu

To cite this article: Halil T. Eyyuboğlu (2016) Correction of amplitude distortions for truncated Bessel beam and SER estimation for 4ASK, Journal of Modern Optics, 63:15, 1438-1443, DOI: 10.1080/09500340.2016.1154197

To link to this article: http://dx.doi.org/10.1080/09500340.2016.1154197

Published online: 25 Feb 2016.

JOURNAL OF MODERN OPTICS, 2016
VOL. 63, NO. 15, 1438–1443
http://dx.doi.org/10.1080/09500340.2016.1154197

Taylor & Francis
Taylor & Francis Group

Correction of amplitude distortions for truncated Bessel beam and SER estimation for 4ASK

Halil T. Eyyuboğlu

Department of Electronic and Communication Engineering, Çankaya University, Ankara, Turkey

ABSTRACT

We apply amplitude corrections to a truncated Bessel beam that has propagated through turbulent atmosphere modelled by random phase screens. These corrections are realized via transmitting an unmodulated beam in parallel to the one carrying the 4 amplitude shift keying (ASK) modulated message signal. On the receiver side, the amplitude corrections are obtained by dividing the intensity of the unmodulated beam by its free space equivalence. The corrections are then used to restore the amplitude distortions of the beam carrying the 4ASK modulated message signal and in the determination of decision boundaries for the received 4ASK symbols. The success of the system is visually inspected by comparing the received intensity profiles before and after the application of corrections. Furthermore, simulation analysis of symbol error rate (SER) is made, where the proposed set-up is found to be quite insensitive to wavelength difference between the unmodulated and modulated beams. On the other hand, the difference in the structure constant values of these two beams seems to have profound effect on system performance.

ARTICLE HISTORY
Received 22 October 2015
Accepted 8 February 2016

KEYWORDS
4ASK; truncated Bessel beam; random phase screen; turbulence

1. Introduction

Correction of amplitude distortions of a beam, that has propagated through turbulent atmosphere, has been the subject of numerous investigations. Such corrections help to restore the beam profile near to its free space equivalent. This way, it becomes much easier to identify decision boundaries and thus particularly in the case of intensity modulations, improved error performance is obtained.

These corrections are examined within the broader context of adaptive optics, where the corrections are achieved by the removal of lower order Zernike polynomials that represent the essential aberrations in the wave front such as piston, tilt, focus, astigmatism and coma [1,2]. The application of such corrections is observed to bring about substantial reductions in error rates of optical communication systems. The related theoretical and experimental results are published in [3,4]. In [5], the application of wave front sensing and adaptive optics to strong turbulence conditions is investigated, where it is stressed that amplitude fluctuations (rather than phase fluctuations) heavily dominate in such situations. A simple analytic model of adaptive optics system that is to be used in a downlink free space optical link is developed and tested in [6]. The use of phase compensation is discussed in [7] for various turbulence conditions. The free space optical link budget estimation is made in [8], where it is stated that adaptive optics compensation of turbulence-induced phase perturbations is limited by Rayleigh range, directly proportional to the square of the aperture opening and inversely proportional to the wavelength of operation. A simplified, namely sensorless adaptive optics system that would provide reduced complexity, size and cost is investigated in [9]. It is shown in [10] that the wave front sensor alignment and calibration can lead to successful data collection on the characterization of atmospheric turbulence. By employing coherent detection and different modulation schemes such as ASK, PSK and FSK, the improvement of the bit error rate is exhibited in [11] against the rising number of Zernike mode correction for weak, moderate and strong turbulence conditions. The feasibility of bidirectional transmission of 100 Gb/s data rates is demonstrated in [12], based on the utilization of adaptive optics pre and post turbulence compensated multiple orbital angular momentum beams. The bit error rate performance of a coherent QPSK modulation operation over a maritime atmospheric link is evaluated in [13], where it is shown that adaptive optics system compensating for both the amplitude and phase distortions can achieve drastic improvement, approaching the turbulence free levels. In

CONTACT Halil T. Eyyuboğlu h.eyyuboglu@cankaya.edu.tr

[14], preliminary results of an adaptive optics system are presented for satellite to ground optical link also incorporating some horizontal path transmission as well.

In the current paper, we test the performance of an optical communication system equipped with amplitude correction capabilities. For this, we benefit from the random phase screen approach. Initially amplitude corrections that are to be applied over the transverse receiver plane are deduced, these are then used to determine the decision boundaries of the 4ASK symbols for detection. Finally SER evaluations are made.

2. Theoretical background

2.1. Modelling amplitude corrections

In Rytov theory, the received field, $u_{rt}\left(r_x, r_y, L\right)$, of a beam which has traversed a distance of L through atmospheric turbulence can be expressed as [1]

$$u_{rt}\left(r_x, r_y, L\right) = u_{rfs}\left(r_x, r_y, L\right)\exp\left[\psi\left(r_x, r_y, L\right)\right] \quad (1)$$

In the above representation, $\left(r_x, r_y\right)$ are the transverse receiver plane coordinates, $u_{rfs}\left(r_x, r_y, L\right)$ stands for the free space field, whereas the effects of the turbulence are accumulated in the complex phase term of $\psi\left(r_x, r_y, L\right)$, which in turn can be split as

$$\psi\left(r_x, r_y, L\right) = \psi_r\left(r_x, r_y, L\right) + j\psi_i\left(r_x, r_y, L\right) \quad (2)$$

On the receiver side, scintillation is created by intensity fluctuations. Using Equations (1) and (2), the received intensity, $I_{rt}\left(r_x, r_y, L\right)$ becomes

$$\begin{aligned} &I_{rt}\left(r_x, r_y, L\right) \\ &= u_{rt}\left(r_x, r_y, L\right)u_{rt}^{*}\left(r_x, r_y, L\right) \\ &= u_{rfs}\left(r_x, r_y, L\right)u_{rfs}^{*}\left(r_x, r_y, L\right)\exp\left[2\psi_r\left(r_x, r_y, L\right)\right] \\ &= I_{rfs}\left(r_x, r_y, L\right)\exp\left[2\psi_r\left(r_x, r_y, L\right)\right] \end{aligned} \quad (3)$$

where $I_{rfs}\left(r_x, r_y, L\right)$ is the free space intensity. Equation (3) demonstrates that intensity fluctuations in $I_{rt}\left(r_x, r_y, L\right)$ will solely arise from the real part of the complex phase, which will be given by

$$\psi_r\left(r_x, r_y, L\right) = 0.5\ln\left[\frac{I_{rt}\left(r_x, r_y, L\right)}{I_{rfs}\left(r_x, r_y, L\right)}\right] \quad (4)$$

For an optical communication system operating at a fixed distance of L and a known transmitted beam, the receiver can easily evaluate $I_{rfs}\left(r_x, r_y, L\right)$ from the known analytic formulations. $I_{rt}\left(r_x, r_y, L\right)$ meanwhile can be measured over the related optical surface by a CCD camera or by some other means. This way, it is possible to determine the values of the real part of the complex phase and its distribution over the receiver area.

In order to assess how many samples of $\psi_r\left(r_x, r_y, L\right)$ will be required for a successful application of amplitude corrections, we assume that the transmitter has a symbol rate of 2 Gsym/s and the photo detector has a response time of 1 ps. Consequently, we can safely assert that an averaging over 500 samples of $\psi_r\left(r_x, r_y, L\right)$ will be sufficient.

It is important to realize that the received field of Equation (1) will experience amplitude fluctuations due to $\psi_r\left(r_x, r_y, L\right)$ as well as phase fluctuations due to $\psi_i\left(r_x, r_y, L\right)$. Here we only need to take into account $\psi_r\left(r_x, r_y, L\right)$, since the photo detector converts the optical intensity integrated over the receiver aperture (power) into electrical current and secondly, our optical communication system will employ amplitude shift keying (ASK), thus phase changes in the optical beam will play no role in the detection process. Besides, it is the amplitude fluctuations that are important in strong turbulence regimes [5]. Such is the case in this paper.

2.2. Adjusting the 4ASK constellation

The constellation arrangement of the 4PSK modulation scheme that is to be used in our simulations is illustrated in Figure 1. Here, the spacing between the ends of the signal vectors (symbols) is made equal on optical power basis with the smallest normalized signal vector being at an amplitude level of $0.1^{0.5}$, while the largest signal vector is placed at an amplitude level of unity.

In this work, source beam is selected to be a Bessel beam whose field expression is given by

$$u_s\left(s_x, s_y\right) = J_0\left[a_B\left(s_x^2 + s_y^2\right)^{0.5}\right] \quad (5)$$

where $\left(s_x, s_y\right)$ are the transverse source plane coordinates, a_B is the width parameter. $u_s\left(s_x, s_y\right)$ will become truncated due to finite dimensions of the source plane. When modulated by one of the signal vectors of 4ASK constellation, the source beam becomes

$$u_{sm}\left(s_x, s_y\right) = \mathbf{s_m}J_0\left[a_B\left(s_x^2 + s_y^2\right)^{0.5}\right] \quad (6)$$

where $\mathbf{s_m} = \{\mathbf{s_1}, \mathbf{s_2}, \mathbf{s_3}, \mathbf{s_4}\} = \{0.1^{0.5}, 0.4^{0.5}, 0.7^{0.5}, 1\}$. The width parameter, is set to $a_B = 43.63\ \mathrm{m}^{-1}$. This way, on a square source plane with a side length of 40 cm, the power of the source beam becomes 10 mW. Note that this is also the maximum power during ASK modulation, when $\mathbf{s_m} = \mathbf{s_4} = 1$.

2.3. Adjusting decision boundaries on receiver side

Although the receiver has knowledge of the modulation type and the associated signal constellation used in the transmitter, this knowledge on its own is not sufficient to establish the decision boundaries for correct detection. For this, the receiver has to be trained with a known transmitted sequence. This way, a constellation diagram similar to Figure 1 will appear, where the decision boundaries can be marked, according to the characteristics of the propagation medium. In our case, the propagation distance is kept constant at $L = 3$ km, so factors affecting the markings of the decision boundaries are wavelength and turbulence level, i.e. the structure constant, C_n^2. In our simulations, two consecutive 500 runs were made. In the first one, the averaged values of $\psi_r\left(r_x, r_y, L\right)$ were drawn up. Then with the insertion of $\psi_r\left(r_x, r_y, L\right)$ values into the received field, amplitude corrected decision boundary markings were determined. This was done by calculating the average photo detector current under the assumption of transmitter sending $\mathbf{s_4}$ constantly, then scaling this in ratios of 0.1, 0.4, 0.7 for the other symbols, $\mathbf{s_1}, \mathbf{s_2}, \mathbf{s_3}$ as shown in Figure 1. Finally the midpoints between these symbols are marked as decision boundaries. A typical example is exhibited in Figure 2.

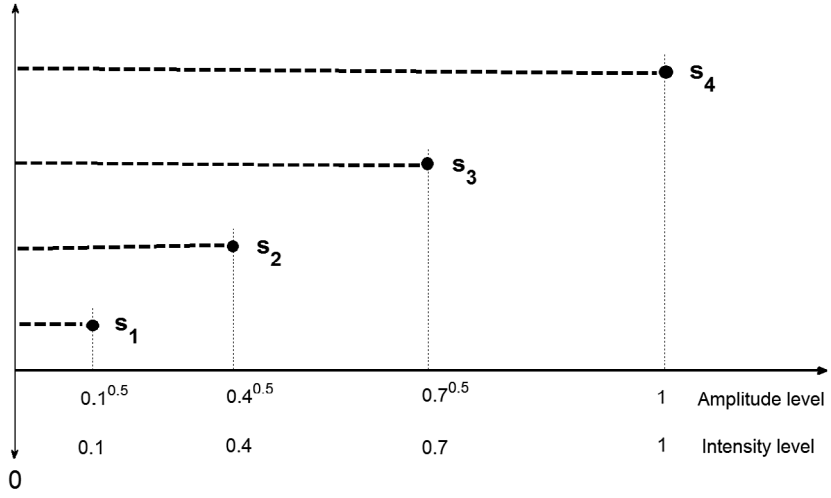

Figure 1. 4ASK signal vector constellation on the source plane.

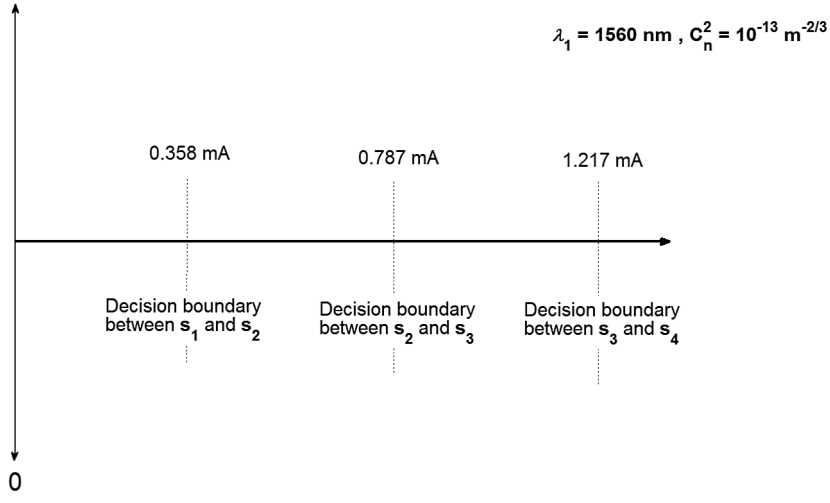

Figure 2. Decision boundaries of 4ASK symbols on receiver side at $\lambda_1 = 1560$ nm and $C_n^2 = 10^{-13}\ \mathrm{m}^{-2/3}$.

2.4. Parameter settings for random phase screen set-up

To ensure the reliability of our results, precautions are taken so that the random phase screen set-up is able to cope with strong turbulence conditions. This is done by choosing the number of grid points on source and receiver planes to be 1024. The number of intermediate planes between the source and the receiver is taken to be 20. The source and the receiver plane dimensions are set to be 40 × 40 cm and 1.024 × 1.024 m, respectively. The receiver aperture has a square opening of 14 × 14 cm. The amplitude correction data is collected within wavelength range of 1530–1580 nm. 4ASK transmission is carried out at a wavelength of 1550 nm, the propagation distance is kept constant at $L = 3$ km, while the structure constant, C_n^2 is varied in the range 10^{-14} $m^{-2/3}$ to 10^{-12} $m^{-2/3}$. With these numeric quantities, it is easy to verify that our system will be operating under strong turbulence conditions with the entire set of constraints specified in [15,16] being well satisfied.

The effective functioning of our amplitude corrections implemented via the real part of the complex phase, $\psi_r\left(r_x, r_y, L\right)$, is displayed in Figure 3. There, Plot A gives the source plane intensity, while Plot B provides the corresponding receiver plane intensity under the conditions of free space propagation. Plot C illustrates the distorted intensity which is obtained after the source plane intensity of Plot A has passed through the turbulent atmosphere. Comparing Plots B and C, it is easy to conclude that decisions based on the intensity Plot C would definitely lead to several errors, unless amplitude corrections are applied. In this sense, Plot D clearly shows that the application of the amplitude corrections successfully removes most of fluctuations caused by turbulence, restoring the distorted received intensity profile nearly to the shape of the free space intensity, thereby offering the possibility of improved error performance. Here beam wander effects are discarded. It is worth noting that the values of $\psi_r\left(r_x, r_y, L\right)$ must be retrieved from the parallel transmission of unmodulated source beam at a wavelength λ_1, which is different from the wavelength λ_2 that is used in the transmission of 4ASK modulated message signal. This way, the amplitude correction data will have to be updated at regular time intervals, possibly at least once within the coherence time of turbulence atmosphere, which is reported to be on the order of ms [17,18]. The related functional block diagram of the optical communication system incorporating amplitude correction arrangement is displayed in Figure 4. As seen from this figure, there exist two links between the transmitter and

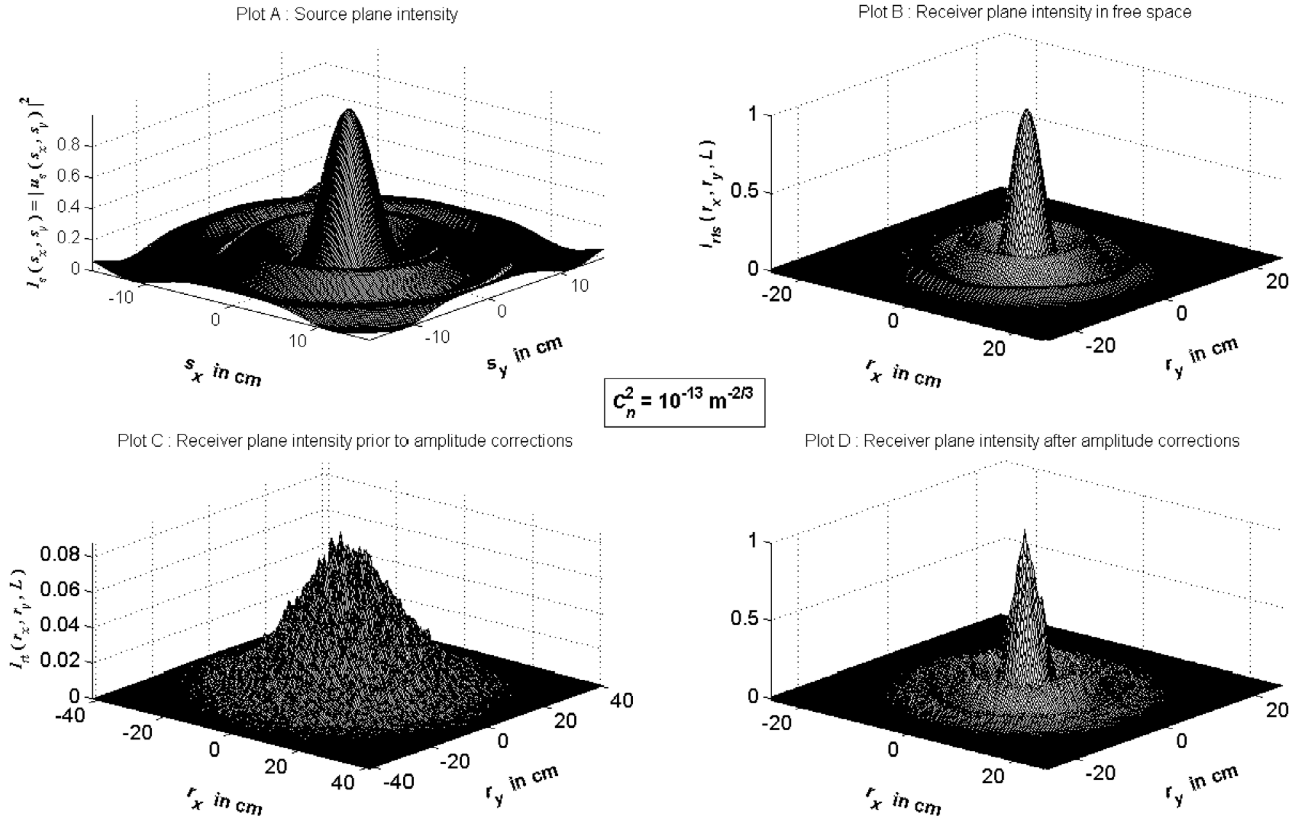

Figure 3. Graph illustrating the effect of amplitude corrections.

the receiver, where the upper link, Link 1, will carry the unmodulated source beam, thus any modulations imposed on the received beam of this link will entirely be due to the characteristics of the turbulent atmosphere. As shown in Figure 4, such modulations will help retrieve the real part of the complex phase $\psi_r\left(r_x, r_y, L\right)$ that can be used in the amplitude corrections in the lower part of the link, Link 2, where the actual message transmission is taking place.

3. SER results and discussions

In this section, we report the results of symbol error rate (SER) runs. Looking at Figure 4, we understand that the amplitude corrections are realized through some wavelength division multiplexing. To this end, the characteristics of turbulent atmosphere measured at λ_1 is providing the amplitude corrections for a beam that has propagated through the same random medium, but this time at λ_2. To assess, how the numeric difference between λ_1 and λ_2 will

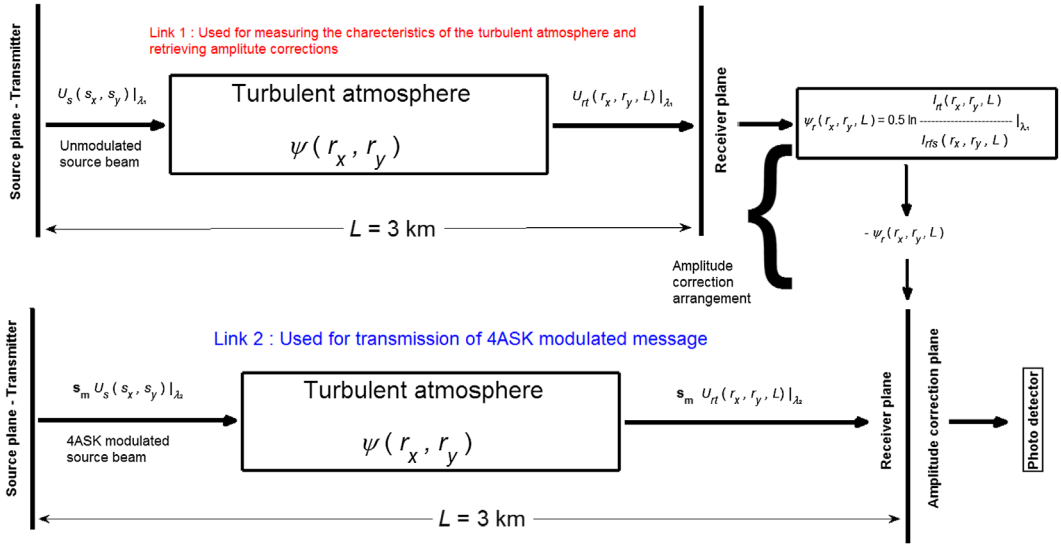

Figure 4. Block diagram illustration of the optical communication system incorporating the amplitude correction arrangement. (The color version of this figure is included in the online version of the journal.)

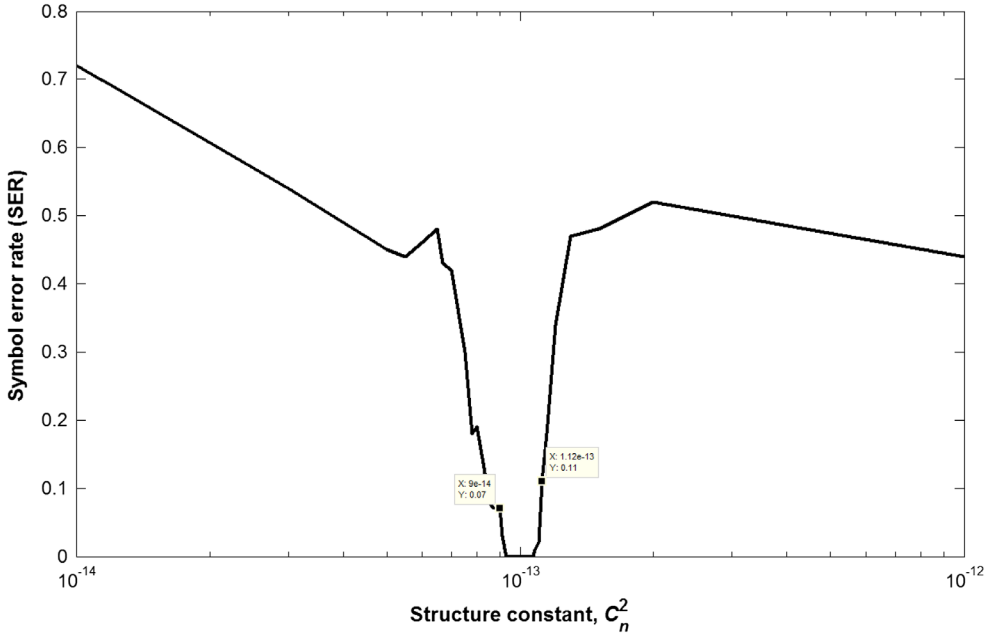

Figure 5. SER variation against the structure constant, C_n^2.

affect the SER performance, we kept λ_2 fixed at 1550 nm and varied λ_1 in the range 1530–1580 nm. This wavelength span covered both the amplitude correction data, i.e. $\psi_r\left(r_x, r_y, L\right)$ and the decision boundaries of Figure 2. Due to excessive time involved in these computations, our tests were limited to 3000 symbol transmissions. No errors were found in these tests. This means that the error originating from the use of a separate wavelength in the range 1530–1580 nm to correct the amplitude distortions of a 4ASK transmission at 1550 nm is somewhere below 3×10^{-3}. Next we report the results of the sensitivity of amplitude corrections against variation in the structure constant, C_n^2. For this, in Link 1, $\psi_r\left(r_x, r_y, L\right)$ values of $\lambda_1 = 1560$ nm and $C_n^2 = 10^{-13}$ m$^{-2/3}$ were kept constant, while for the lower link, Link 2, of Figure 4, $\lambda_2 = 1550$ nm and C_n^2 was allowed to vary in the range 10^{-14} m$^{-2/3}$ to 10^{-12} m$^{-2/3}$. Results are displayed in Figure 5. As seen from this figure, deviations of the structure constant values from $C_n^2 = 10^{-13}$ m$^{-2/3}$ in the turbulent atmosphere through which the 4ASK symbols have been transmitted, have profound effects on SER. To illustrate this point, two data cursor markings appear in Figure 5, one to the left and the other to the right of the central structure constant value of $C_n^2 = 10^{-13}$ m$^{-2/3}$. Accordingly, we witness that as C_n^2 drops by 10%, SER rises from zero (or theoretically from 3×10^{-3}) to 7×10^{-2}. For the right-hand side of the curve, we see that if C_n^2 is increased by 12%, SER will become 11×10^{-2}. From the rapidly rising slopes on either side of $C_n^2 = 10^{-13}$ m$^{-2/3}$, we understand that the amplitude correction mechanism will serve correctly only within a narrow region around this structure constant central value.

The scenario contemplated for Figure 5 is a realistic one, since in practice, the computation of $\psi_r\left(r_x, r_y, L\right)$ will require finite time and there will be a physical response time of the amplitude correction plane. Hence, time delays are inevitable in the application of the amplitude corrections of Link 1 to the 4ASK transmission of Link 2. During such time delays, it is quite probable that the characteristics of the turbulent atmosphere will change and consequently, the structure constant values, C_n^2 will drift. The horizontal axis of Figure 5 is intended to represent such drifts. For commercially available correctors such as SLM devices, the response time is quoted to be in the order of ms [19].

4. Conclusion

We constructed and tested the performance of an amplitude correction mechanism devised for an optical system operating with a 4ASK modulated truncated Bessel beam. The propagation medium of turbulent atmosphere was modelled by random phase screen. Initially runs were made with unmodulated beam at different wavelengths and structure constant values to acquire the amplitude corrections that would be utilized in the restoration of amplitude distortions of the received beam. In subsequent runs, such corrections allowed the determinations of the decision boundaries of the received 4ASK symbols. SER measurements were then made for the wavelength difference between the beams carrying the amplitude corrections and the actually transmitted message. There, no appreciable performance degradation was found. When however, a difference in the structure constant was created, it was seen that SER would increase rapidly even for a 10% deviation in the value of the structure constant. Bearing in mind that the coherence time of atmospheric turbulence is in the order of ms, it would be desirable to have an amplitude correction device which could replenish itself within μs. Of course for practical correctors, there would be size and number of grids (pixel) limitations as well. The present results were obtained, taking into account no such limitations.

Disclosure statement

No potential conflict of interest was reported by the author.

References

[1] Andrews, L.C.; Phillips, R.L. *Laser Beam Propagation through Random Media*, 2nd ed.; SPIE Press: Bellingham, WA, 2005.
[2] Tyson, R.K. *Appl. Opt.* **1982**, *21*, 787–793.
[3] Tyson, R.K. *J. Opt. Soc. Am. A*. **2002**, *19*, 753–758.
[4] Tyson R.K.; Canning, D.E.; Tharp, J.S. *Opt. Eng.* **2005**, *44*, 096002-1–096002-6
[5] Mackey, R.; Dainty, C. *Proc. SPIE*. **2005**, *5827*, 23–29.
[6] Zocchi, F.E. *Opt. Commun.* **2005**, *248*, 359–374.
[7] Schwartz N.H.; V′edrenne, N.; Michau, V.; Velluet, M.T.; Chazallet, F. *Proc. SPIE*. **2009**, *7200*, 72000J-1–11.
[8] Stotts, L.B.; Kolodzy, P.; Pike, A.; Graves, B.; Dougherty, D.; Douglass, J. *Appl. Opt*. **2010**, *49*, 5333–5343.
[9] Sharma, S. *Int. J. Electron.* **2012**, *99*, 417–436.
[10] Sergeyev, A.V.; Levin, E.; Roggemann, M.C. *Proc. SPIE*. **2012**, *8408*, 84080R-1–7.
[11] Liu, C.; Chen, S.; Li, X.Y.; Xian, H. *Opt. Express*. **2014**, *22*, 15554–15563.
[12] Ren, Y.; Xie, G.; Huang, H.; Ahmed, N.; Yan, Y.; Li, L.; Bao, C.; Lavery, M.P.J.; Tur, M.; Neifeld, M.A.; Boyd, R.W.; Shapiro, J.H.; Willner, A.E. *Optica*. **2014**, *1*, 376–382.
[13] Li, M.; Cvijetic, M. *Appl. Opt.* **2015**, *54*, 1453–1462.
[14] Gregory, M.; Troendle, D.; Muehlnikel, G.; Heine, F.; Meyer, R.; Lutzer, M.; Czichy, R. *Proc. SPIE*. **2013**, *8610*, 861004-1–13.
[15] Rao, R. *Appl. Opt.* **2008**, *47*, 269–276.
[16] Eyyuboğlu, H.T. *Appl. Opt.* **2014**, *53*, 2290–2296.
[17] Greenwood, D.P. *J. Opt. Soc. Am.* **1977**, *67*, 390–393.
[18] Kellerer A. *Assessing time scales of atmospheric turbulence at observatory sites*, Universite Paris Diderot: Paris, 2007.
[19] *Phase Spatial Light Modulator LCO-SLM*, Chapter 12.https://www.hamamatsu.com/resources/pdf/ssd/e12_handbook_lcos_slm.pdf (accessed Oct 15, 2015.